HHS Public Access

Author manuscript

Pharmacol Res. Author manuscript; available in PMC 2020 March 01.

Published in final edited form as:

Pharmacol Res. 2019 March ; 141: 276–290. doi:10.1016/j.phrs.2019.01.015.

Formyl peptide receptor-1 activation exerts a critical role for the dynamic plasticity of arteries via actin polymerization

Camilla F. Wenceslau[1,2], **Cameron G. McCarthy**[1,2], **Theodora Szasz**[2], **Fabiano B. Calmasini**[2], **Mykola Mamenko**[2], and **R. Clinton Webb**[2]

[1]Department of Physiology and Pharmacology, University of Toledo College of Medicine & Life Sciences, Toledo OH, USA.

[2]Department of Physiology, Augusta University, Augusta GA, USA.

Abstract

Several human diseases, include cancer and stroke are characterized by changes in immune system activation and vascular contractility. However, the mechanistic foundation of a vascular immuno-physiology network is still largely unknown. Formyl peptide receptor-1 (FPR-1), which plays a vital role in the function of the innate immune system, is widely expressed in arteries, but its role in vascular plasticity is unclear. We questioned why a receptor that is crucial for immune defense, and cell motility in leukocytes, would be expressed in vascular smooth muscle cells (VSMCs). We hypothesized that activation of FPR-1 in arteries is important for the temporal reorganization of actin filaments, and consequently, changes in vascular function, similar to what is observed in neutrophils. To address our hypothesis, we used FPR-1 knockout and VSMCs lacking FPR-1. We observed that FPR-1 activation induces actin polymerization in wild type VSMCs. Absence of FPR-1 in the vasculature significantly decreased vascular contraction and induced loss of myogenic tone to elevated intraluminal pressures via disruption of actin polymerization. Actin polymerization activator ameliorated these responses. In conclusion, we have established a novel role for FPR-1 in VSMC contractility and motility, similar to the one observed in sentinel cells of the innate immune system. This discovery is fundamental for vascular immuno-pathophysiology, given that FPR-1 in VSMCs not only functions as an immune system receptor, but it also has an important role for the dynamic plasticity of arteries.

Graphical Abstract:

Corresponding Author: Camilla Ferreira Wenceslau, Ph.D., Assistant Professor, Department of Physiology and Pharmacology, The University of Toledo College of Medicine & Life Sciences Laboratory of Vascular Biology (LVB), http://www.utoledo.edu/med/depts/physpharm/faculty/camillawenceslau.html, 3000 Transverse Drive, Toledo, Ohio 43614-2598, Phone#: 419.383.5307, Camilla.Wenceslau@utoledo.edu.

Author Contributions

All authors approved the final version of the manuscript. **C.F.W.** conceived the experiment design, analyzed the data and wrote the manuscript. **C.G.M.,** support the interpretation of the data and performed the experiments; **F.B.C., T.S. and M.M.** performed the experiments. **R.C.W.** revised it critically for important intellectual content.

Conflict of Interest

None declared

Schematic proposing that formyl peptide receptor-1 (FPR-1) play a role in the vascular function. Formyl peptide receptor (FPR-1), an innate immune system receptor, mediates vascular plasticity during physiological conditions. Upon activation (by agonist or stretch), FPR-1 triggers actin polymerization via an integrated network with Cav 1.2 and RhoA. Future studies are needed to dissect the mechanisms associated with FPR-1 activation and its functions as a mechanosensor-like receptor and vascular-immuno network during perturbations.

Keywords

Formyl Peptide Receptor-1; Actin Polymerization; Vascular Contractility

Introduction

The vascular wall and its compounds, including endothelial cells, are not static (Cipolla *et al.*, 2002; Prasain *et al.*, 2009, Walsh & Cole, 2013). It was once accepted that the vascular smooth muscle cells (VSMCs) cytoskeleton remains stationary during a contractile event (Cipolla *et al.*, 2002). Now, it is recognized that the cytoskeleton displays a highly dynamic process characterized by polymerization and depolymerization of the cytoskeleton based upon cellular demand (Walsh & Cole, 2013). For example, pressure-induced actin polymerization in VSMCs is a mechanism underlying myogenic contraction (Cipolla *et al.*, 2002).

Recent evidence indicates that prolonged vasoconstriction of conductance and resistance arteries involves VSMCs actin polymerization, through activation of small GTPases (Staiculescu *et al.*, 2013) and a subsequently transition to a more solid rheology (Rembold *et al.*, 2007). Actin polymerization occurs in two steps, nucleation and elongation. Nucleation occurs when three actin monomers bind together and provide a site for elongation. Elongation occurs when ATP-bound globular (G)-actin binds and grows to form filamentous (F)-actin (Prasain *et al.*, 2009). For both mechano-transduction pathway and agonist-induced changes in actin polymerization, the RhoACdC42 pathway has been reported to be involved (Yamin & Morgan, 2012; Moreno-Domínguez *et al.*, 2013). Interestingly, actin organization has also been observed to be important for the function of L-type calcium channels (Cav 1.2). Accordingly, disruption of actin polymerization by cytochalasin D dramatically decreased Cav 1.2 current in VSMCs (Nakamura *et al.*, 2000). In an elegant study performed by Drs. Cole and Walsh's group (Moreno-Domínguez *et al.*, 2013), it was observed that PKC-evoked actin polymerization also contributes to the myogenic response of skeletal muscle resistance arteries. Actin polymerization and myosin phosphorylation are independent events (Walsh & Cole, 2013), but both actin filament formation and myosin phosphorylation are required for smooth muscle contraction (Walsh & Cole, 2013).

Innate immune cell movement is coordinated spatially as well as temporally by mechanical changes in the cytoskeleton which results in actin polymerization (Ananthakrishnan & Ehrlicher, 2007). One of the most powerful signaling pathways that induces actin polymerization and neutrophil movement is mediated by formyl peptide receptor (FPR-1) activation (Norgauer *et al.*, 1994; Le *et al.*, 2001). Stimulation of FPR-1 in neutrophils

causes polymerization of actin within 10 seconds. In contrast to the cytokine IL-8 receptor, FPR-1 activation also triggers Ca^{2+} influx in neutrophil (Norgauer *et al.*, 1994). The FPR family was originally identified by its ability to bind N-formyl peptides such as N-formylmethionine, produced by bacterial degradation (Le *et al.*, 2001). Interestingly, mitochondria carry hallmarks of their bacterial ancestry and one of these hallmarks is that these organelles use an N-formyl-methionyl-tRNA as an initiator of protein synthesis (Le *et al.*, 2001; Wenceslau *et al.*, 2015). Consequently, both mitochondrial and bacterial-produced peptides have a formyl group at their N-terminus. N-formyl peptides, regardless of origin, are recognized by FPR-1 as pathogens and thus play a role in the initiation of inflammation. Any injury that causes cell lysis *in vivo* leads to release of damage-associated molecular patterns (DAMPS), including mitochondrial N-formyl peptides (F-MITs). Our group was the first to observe that FMITs were increased in trauma patients and in animals that underwent sterile trauma, and these peptides were able to activate FPR-1 leading to cardiovascular collapse (Wenceslau *et al.*, 2015; 2016). More recently, we also observed that FPR-1 is not only expressed in sentinel cells (cells that are important for the host defense, such as leukocytes), but also in endothelial cells and VSMCs, as well as airways (trachea, bronchus and bronchiole). Functionally, activation of FPR-1 *in vitro* induced a slow and sustained contraction in a concentration-dependent manner in airways and vascular leakage in arteries from naïve rats (Wenceslau *et al.*, 2015; 2016). Systemic FPR-1 activation leads to sepsis-like symptoms, including lung inflammation and formation of neutrophil extracellular traps (NETs) in the lungs (Wenceslau *et al.*, 2016).

Therefore, based on this previous knowledge, in the present study we wanted to understand the role of FPR-1 in VSMCs. We questioned why a receptor that is crucial for immune defense, and cell motility in leukocytes, would be expressed and functional in VSMCs? We hypothesized that activation of FPR-1 in arteries is important for the temporal reorganization of actin, and consequently, changes in vascular function, similar to what is observed in neutrophils. We observed that F-MITs rapidly induce actin polymerization via FPR-1 activation in VSMCs. On the other hand, the absence of FPR-1 in the vasculature of knockout mice significantly decreased vascular contraction and induced loss of myogenic tone to elevated intraluminal pressures. The use of a potent inducer of actin polymerization ameliorated these responses. Therefore, we have established a novel role for FPR-1 in VSMCs contractility and motility, similar to the one observed in sentinel cells of the innate immune system, such as neutrophils. This discovery is fundamental for vascular immuno-pathophysiology, given that FPR-1 in VSMCs not only functions as an immune system receptor and danger signal sensor by detecting foreign pathogens and DAMPs in the bloodstream (Wenceslau *et al.*, 2015; 2016), but it also has an important role for the dynamic plasticity of arteries.

Methods

Ethical Approval

All procedures were performed in accordance with the Guide for the Care and Use of Laboratory Animals of the National Institutes of Health (NIH) (Grundy D, 2015) and were

reviewed and approved by the Institutional Animal Care and Use Committee of the Augusta University -GA, and the University of Toledo College of Medicine -OH.

Animals

Male, 10–14-week-old FPR-1 knockout (KO) and wild-type (WT) mice with C57BL/6 genetic background were used. FPR-1 KO animals were kindly donated from Charles R. Mainhart, PhD, NIH National Institute of Allergy and Infectious Diseases/Taconic Repository CORE. The animals were maintained on a 12:12 hour light-dark cycle with both standard chow and water ad libitum. For cell culture procedures and vascular reactivity experiments, mice used were sacrificed by isoflurane (5%) inhalation and exsanguination.

Blood Pressure Measurements

Radiotelemeter implantation surgery was performed under anesthesia with 3% isoflurane. Animals were placed on their backs on a heated pad (37°C) and ~1 cm midline incision was made in the skin of the neck of the mouse with a scalpel. A subcutaneous space was created on the left side of the incision by carefully separating the skin from the underlying connective tissue. Subsequently, a skin incision (~1.5 cm) was made in the dorsal left side between the scapulae to accommodate the radiotelemeter device (PA-C10, Data Sciences International, St. Paul, MN). The left carotid artery was located and cleaned from the surrounding tissue and the vagus nerve. Non-absorbable 5–0 suture was used for cranial permanent ligature and temporary caudal occlusion of the left carotid artery. A small incision was made in the wall of the artery to introduce and advance the catheter. The catheter was secured to the carotid artery with silk knots and the skin incision was closed. Animals were allowed at least 7 days to recover postoperatively. Systolic pressure, diastolic pressure (SBP), mean arterial pressure, pulse pressure, heart rate and activity (movement) were recorded at a sampling rate of 10 seconds each 10-minute interval.

Vascular function and structural measurements

Isometric—The kidneys, mesenteric arcade and aorta were carefully removed. Second and third-order branches from mesenteric arteries [internal diameter μm; WT: 180±10 (n=9) vs. FPR-1 KO: 181±9.6 μm (n=9), t test, $p>0.05$] and intrarenal arteries [inferior segmental arteries, internal diameter μm; WT: 225±12 (n = 8) vs. FPR-1 KO: 244 ± 11 μm (n=8), t test, $p>0.05$] and aorta were removed and cleaned of surrounding tissue in cold Krebs-Henseleit solution (KHS, in mmol/l): NaCl 118; KCl 4.7; NaHCO3 25; CaCl2.2H2O 2.5; KH2PO4 1.2; MgSO4.7H2O 1.2; EDTA 0.01; glucose 11. Segments (in length: 2 mm for resistance arteries and 3 mm for aorta) were mounted in a wire and pin myograph chamber (Danish Myo Tech, model 610M; JP-Trading I/S), respectively, for isometric tension recordings, as described previously (Wenceslau *et al.*, 2014). Briefly, for resistance arteries two steel wires (40 μm diameter) were introduced through the lumen of the segments and mounted according to the method described by Mulvany and Halpern (1977). After a 15-min equilibration period in oxygenated KHS at 37°C and pH 7.4, segments were stretched to their optimal lumen diameter for active tension development. This was determined based on the internal circumference/wall tension ratio of the segments by setting the internal circumference, L_0, to 90% of what the vessels would have if they were exposed to a jo

tension equivalent to that produced by a transmural pressure of 100 mmHg (L100) (Wenceslau *et al.*, 2014). The diameter (I1) was determined according to the equation I1 = L1/π, using specific software for normalization of resistance arteries (DMT Normalization Module; ADInstruments).

Segments were washed with KHS and left to equilibrate for 20 min. Vessel contractility and endothelium viability were then tested by an initial exposure to a high-K^+ (120 mmol/l) solution and by using acetylcholine (3 μM) in vessels contracted with phenylephrine (3 μM) respectively. Arteries then rested for 30 min, after which they were subjected to one of the following two protocols: 1) concentration-response curves to phenylephrine (10 nmol/l to 1 μmol/l) were performed in the absence or presence of cytochalasin B (CYTO B, 1 μmol/l, 45 min incubation) (inhibits both the rate of actin polymerization and the interaction of actin filaments in solution); jasplakinolide (JASP, 0.1 μmol/l; 45 min incubation) (promotes actin-stabilizing and inhibits depolymerizing) and Rho Activator II (CN03, 1.25 μg/ml, 2 hours incubation); 2) concentration-response curves to BAY 8644 (10 nmol/l to 10 μmol/l) were performed in the presence of elevated K^+ (26.2 mM) (Storm & Webb, 1993).

Isobaric—The third- and fourth-order branches from mesenteric resistance arteries (MRA) were carefully removed. The structural and mechanical properties were evaluated using pressure myograph as previously described (Briones *et al.*, 2007).

The 2 mm segments were bathed in filtered KHS and cannulated at both ends in an arteriography using a glass microcannula (75–100 μm diameter, Living System Instrumentation Inc) and then knotted with surgical nylon suture. Subsequently, vessel length was adjusted to maintain the vessel walls parallel at increasing pressures. Flow in the vessel was generated through the distal pipette with a peristaltic pump. Intraluminal pressure was then raised to 120 mmHg, and again the vessel length was adjusted. The segment was set to a pressure of 60 mmHg (no flow) and allowed to equilibrate for 20 min at 37°C in KHS, gassed with a mixture of 95% O_2 and 5% CO_2. Afterward, intraluminal pressure was decreased to 0 mmHg. A pressure-diameter curve was obtained by increasing intraluminal pressure in 20 mmHg steps from 0 to 140 mmHg. The same procedure was repeated in Ca^{2+} free-KHS + EGTA (Briones *et al.*, 2007).

Arterial diameter was measured and recorded continuously using a video monitoring system (IonOptix, USA). Internal and external diameters were continuously measured under active and passive conditions (Di0Ca, De0Ca) for 2 min at each intraluminal pressure. The final value used was the mean of the three regions of interest, taken during the last 30s when the artery/lumen diameter reached a steady state (Briones *et al.*, 2007).

Calculation of Myogenic tone, Structural and Mechanical Parameters

Myogenic tone and Structural parameters were calculated or normalized by passive conditions, as previously described:

$$\text{Myogenic tone}\ (\%) = ((\text{Di0Ca} - \text{Di})/\text{Di0Ca}) \times 100)$$

$$\text{Diameter} = (\text{Di}/\text{Di0Ca60mmHg}) \times 100$$

$$\text{Wall thickness (WT)} = (\text{De0Ca} - \text{Di0Ca})/2$$

$$\text{Wall:lumen} = (\text{De0Ca} - \text{Di0Ca})/2\text{Di0Ca}$$

$$\text{Cross-sectional area} = (\pi/4) \times \left(\text{De0Ca}^{2} - \text{Di0Ca}^{2}\right)$$

As Briones *et al.* (2007) described, incremental distensibility represents the percentage of change in the arterial internal diameter for each mmHg change in intraluminal pressure:

$$\text{Incremental Distensibility} = (\Delta\text{Di0Ca}/(\text{Di0Ca} \times \Delta\text{P}) \times 100)$$

Circumferential wall strain (ε) = (Di0Ca - D00Ca)/D00Ca, where D00Ca is the internal diameter at 0 mmHg and Di0Ca is the observed internal diameter for a given intravascular pressure both measured in 0Ca2+-KHS.

Circumferential wall stress (σ) = (P × Di0Ca)/(2WT), where P is the intraluminal pressure (1 mmHg = 1.334 × 103 dynes cm-2) and WT is wall thickness at each intraluminal pressure in 0Ca2+-KHS.

Arterial stiffness is determined by the Young's elastic modulus (E=stress/strain) (Briones *et al.*, 2007). The stress-strain relationship is non-linear; therefore, it is important to obtain a tangential or incremental elastic modulus (Einc) by determining the slope of the stress-strain curve (Einc =δσ/δε) (Briones *et al.*, 2007). Einc was obtained by fitting the stress-strain data from each animal to an exponential curve using the equation: $\sigma = \sigma\text{orig}e^{\beta\varepsilon}$, where σorig is the stress at the original diameter. Taking derivatives on the equation presented earlier, we see that Einc=βσ. For a given σ-value, Einc is directly proportional to β. An increase in β implies an increase in Einc, which means an increase in stiffness (Briones *et al.*, 2007).

Cell culture

Thoracic aortae and intrarenal arteries (diameter < 250 μm) were removed from WT mice, FPR-1 KO mice or Wistar rats. Subsequently, primary VSMCs were isolated and cultured using an enzymatic digestion method (McCarthy *et al.*, 2018). Cells were then grown in a humidified chamber at 37°C, with 5% CO_2, and low glucose Dulbecco's Modified Eagle's Medium (GE Healthcare, Logan, UT, USA) containing 10% fetal bovine serum and 1% penicillin/streptomycin solution (Corning, Manassas, VA, USA). Treatments commenced between passages 3–6, when culture dishes were ≥80% confluent. Twenty-four hours prior to treatments, cells were placed into serum-free media to achieve quiescence.

Intracellular Ca^{2+} imaging

Intracellular calcium levels were assessed using ratiometric Fura-2 fluorescence imaging. In brief, VSMCs were cultured on 5×5 mm coverslips, cut from square 25×25 mm, No. 1 cover glasses (VWR, Radnor, PA, USA) were removed from the culturing medium and incubated with 5 μM Fura-2/AM + 30 μM pluronic acid in Krebs solution for 30 min at +37 °C. After the incubation, the coverslip with VSMC was allowed to wash in Krebs solution for 5–10 min at room temperature to remove the excess of Fura-2/AM. Subsequently, the cells were transferred to an open-top recording chamber (RC-26GLP; Warner Instruments, Hamden, CT, USA) attached to the microscope stage of a Nikon Ti-U inverted microscope (Nikon Instruments, Melville, NY, USA). A 40× Nikon Super Fluor objective was integrated with a Lambda DG-4 light source (Sutter Instrument, Novato, CA, USA) and a CoolSNAP Dyno 2.8 megapixel monochrome CCD camera (Photometrics, Tucson, AZ, USA) controlled by NIS Elements 5.02 Imaging Software (Nikon Instruments, Melville, NY, USA). Fura-2 fluorescent signal was monitored at 510 nm in response to repetitive brief (~100 ms) excitation at 340 and 380 nm every 5 s. Individual cells were selected as regions of interest and the ratio of fluorescent intensities F340/F380, representing $[Ca^{2+}]i$ levels was calculated. No significant Fura-2 bleaching or leakage was detected during the experiments. At least 3 different coverslips were used for each set of experiments. During experiments, cells were perfused with Krebs solution containing normal (5 mM) or high (120 mM) KCl concentrations using a multichannel valve perfusion system (VC-8P eight-channel perfusion valve control system by Warner Instruments, Hamden, CT, USA, or analogue). The amplitude of the response to increased KCl (ΔF) for a given cell was calculated as the difference between the highest value of F340/F380 ratio upon KCl application and the average F340/F380 ratio at the baseline. The onset (τrise) and decay (τdecay) time constants were extracted by fitting the fluorescent ratio trace (for the first response to KCl) with an exponential function: $y=y\_0 + A\_1 \cdot e^{\wedge}(-(x-x\_0)/t\_1)$. Two consecutive responses to elevated KCl were recorded within a 4 min interval, allowing the myocytes to recover in normal KCl Krebs solution. The recovery rate (ΔF Recovery) was estimated as the ratio of the second to the first response amplitudes.

Filamentous and globular actin quantification

The most accurate method of determining the amount of filamentous actin (F-actin) content versus free globular-actin (G-actin) content in a cell population is to use quantitation of F-actin and G-actin cellular fractions (McCarthy *et al.*, 2018). Vascular smooth muscle cells were treated with non-formylated peptides (control) or F-MIT (20 min, 10 μM) in the presence or absence of FPR-1 antagonist (cyclosporine H: CsH, 1 μmol/L and WRW4, 10 μmol/L) and processed according to a G actin: F actin in vivo assay (Cytoskeleton, USA). Briefly, VSMCs were lysed in a detergent-based buffer that stabilizes the G and F forms of actin. Ultracentrifugation was then used to separate them – pelleting the F actin and leaving the G actin in the supernatant. After collecting the G actin, the F actin was depolymerized. Finally, the F and G actin samples were loaded into polyacrylamide gels (10%), separated by SDS-PAGE, and transferred to PVDF membranes, as described above for Western blotting. Known quantities of actin control protein were included as standards. Densitometric analysis was performed by Un-Scan-It (Silk Scientific).

Confocal microscopy

To visualize F actin bundles and α-tubulin, VSMCs were grown in Lab-Tek II Chamber Slide w/Covers (Thermofisher), treated with non-formylated peptides or F-MIT (20 min, 10 μM), and confocal microscopy was performed. After treatment, VSMCs were fixed in 4% paraformaldehyde (Thermofisher) for 10 min and blocked in 1X PBS with 0.01% Triton X-100 (Thermofisher) and 5% horse serum. The slides were then incubated with mouse anti-α-tubulin (1:100; Sigma) primary antibody in 1X PBS and 5% bovine serum albumin (BSA) overnight. Next, slides were incubated with goat anti-mouse IgG (H+L) cross-adsorbed secondary antibody Alexa Fluor 488 (1:200; Thermofisher /A-11008) and rhodamine phalloidin (1:40; Thermofisher /R415) in 1X PBS and 5% BSA for 90 min. Vectashield HardSet Antifade Mounting Medium with DAPI (H-1500) (Vector Laboratories, Inc., Burlingame, CA) was then applied to slides with coverslips. Vascular smooth muscle cells were visualized using a Zeiss LSM 780 Upright confocal microscope (63X objective) (Carl Zeiss MicroImaging, Oberkochen, Germany).

Immunoblotting

Vascular smooth muscle cells were treated with non-formylated peptides or F-MIT (20 min, 10 μM). After treatment, cells were washed with an ice-cold phosphate-buffered saline (PBS) solution. Complete Lysis-M, including phosphatase inhibitor cocktail (PhosSTOP) (both Roche, Indianapolis, IN, USA), was then applied to each plate and allowed to remain on ice for 30 min. Cells were then harvested. Protein concentration was first determined and then equal quantities of protein were loaded into polyacrylamide gels (8–12%) and separated by sodium dodecyl sulfate polyacrylamide gel electrophoresis (SDS-PAGE). Gels were then transferred to polyvinylidene difluoride (PVDF) membranes (Thermofisher). The membranes were blocked with 5 % nonfat dry milk and incubated overnight at 4°C with primary antibodies raised against anti-RhoA (1:2000; Cell Signaling), ROCK (1:1000; Cell signaling), L-type calcium channel (Cav 1.2, 1:500, abcam), PKCα (1:1000, BD Bioscience), AHNAK (1:1000, Thermofisher), pMYPT1^{Thr696} (1:1000, Cell Signaling), MYPT1 (1;1000, BD Transduction). β-actin (1: 40:000, Sigma) was used as the loading control. Densitometric analysis was performed by Un-Scan-It (Version 6.1) (Silk Scientific, USA).

Drugs

Stock solutions of phenylephrine, acetylcholine and RhoA activator II were prepared in distilled water. Jasplakinolide, cytochalasin B, F-MIT and non-formylated peptides were dissolved in dimethyl sulfoxide and Bay K8644 was dissolved in ethanol. All drugs were purchased from Sigma-Aldrich CO (Saint Louis, USA) except for Rho activator II (Cytoskeleton, USA), F-MIT and non-formylated peptides (GenScript, USA).

Statistical analysis

The central hypothesis of the manuscript is that activation of FPR-1 in arteries is important for the temporal reorganization of actin filaments, and consequently, changes in vascular function, similar to what is observed in neutrophils. To address this hypothesis the statistical procedures used included Student’s unpaired t-tests and two-way analysis of variance

(ANOVA). All analyses were performed using data analysis software GraphPad Prism 5.0 (USA, CA). Number (n) of the animals used is indicated in the graphs. Statistical significance was set at $p<0.05$. The data are presented as mean ± SEM.

Results

The absence of FPR-1 decreased both the acute and prolonged-phases of contraction to potassium chloride (KCl) and phenylephrine, as well as caused endothelial dysfunction.

It is well known that during the onset of vasoconstriction there is an increase in intracellular Ca^{2+} which activates myosin light-chain kinase followed by cycling of actin-myosin cross-bridges in VSMCs. Recently, it has been recognized that actin polymerization is also involved in the prolonged phase of vasoconstriction (Staiculescu *et al.*, 2013). To determine if FPR-1 is required for acute and/or prolonged contraction, isometric force was measured in conductance (aorta) and resistance arteries [mesenteric resistance arteries (MRA) and intrarenal arteries - diameter < 300 μm] from FPR-1 KO and WT (C56BL/6) mice. The absence of FPR-1 decreased both the acute-(actin-myosin cross-bridges) as well as the prolonged-phase (actin polymerization) of KCl-induced contraction in all arterial beds studied (Figure 1 A, B and C). Similarly, phenylephrine-induced contraction was decreased in aorta (Figure 1 D and Figure 2 C) and resistance arteries (Figure 2 A and B) from FPR-1 KO animals. These data revel a novel and previously unrecognized role underlying FPR-1 function in vascular contractility.

Pressure-induced myogenic response is lost in arteries lacking FPR-1.

Changes in tension and shear-stress play a critical role in the activation of neutrophils via mechanosensing receptors (Moazzam *et al.*, 1997). In the presence of fluid shear stress, neutrophils rapidly retract lamellipodia, assume a rounded resting state, and decrease G-protein-coupled receptor (GPCR) constitutive activity (Moazzam *et al.*, 1997). Interestingly, it has been shown that shear stress-induced conformational changes in neutrophils occur via FPR, suggesting that this receptor has mechanosensing receptor properties (Mitchell & King 2012). Similarly, small arteries contract in response to increases in intraluminal pressure, known as the myogenic response (Bayliss, 1902; Meininger & Davis, 1992), and this is primarily mediated by mechanosensors. Recently, actin polymerization within VSMCs in response to increased intravascular pressure was recognized as a novel mechanism underlying arterial myogenic behavior (Cipolla *et al.*, 2002). Based on these facts, we hypothesized that FPR-1 would have mechanosensor-like properties, as similar to neutrophils (Makino *et al.*, 2006), and its loss would reduce myogenic response.

FPR-1 KO mice showed a significant reduction in pressure-induced myogenic tone (Figure 3, A, B and C), suggesting that FPR-1 plays an important role in arterial myogenic behavior. Additionally, we observed that FPR-1 KO presented an increased vascular stiffness, as shown by the leftward shift in the stress-strain curve (Figure 4 A) and an increase in the elastic modulus β (Figure 4 C). Also, incremental distensibility at low pressure (< 30 mmHg) was significantly reduced in FPR-1 KO, but no such difference was observed at higher pressures (Figure 4 B). Therefore, just as we hypothesized, FPR-1 KO mice have a reduced myogenic response to increasing intraluminal pressure, which could increase wall

tension and subsequently arterial stiffness. Wall:lumen ratio (Figure 4 D, wall thickness (Figure 4 E) and total collagen (Figure 4 I) were both similar in MRA from WT and FPR-1 KO mice. Intriguing, internal and external diameter and, subsequently, cross-sectional area (CSA) (Figure 4 F, G and H) were decreased in arteries from FPR-1 KO mice, suggesting an inward hypotrophic remodeling.

FPR-1 activation induces VSMCs actin polymerization. In contrast, VSMCs lacking FPR-1 present cytoskeleton disorganization and impaired cell migration.

We further observed that VSMCs from FPR-1 KO present disrupted F-actin and α-tubulin (Figure 5 A). To better understand the role of FPR-1 in VSMCs in the regulation of actin dynamics, we hypothesized that fragments from mitochondria (F-MIT, formylated peptide corresponding to the NH2-terminus of mitochondria ND6) bind to FPR-1 and lead to actin polymerization in VSMCs, similar to neutrophils activated by bacterial fragments. For this, VSMCs isolated from aorta by enzymatic digestion were treated with F-MIT (20 min, 10 μM) or nonformylated peptide (control) in the presence or absence of a cocktail of FPR antagonists (Cyclosporine H: CsH, 1 μmol/L and WRW4, 10 μmol/L). We observed that F-MIT induced VSMCs actin polymerization via a shift in the F:G equilibrium in favor of F-actin (Figure 5 B).

Because cell migration is driven by continuous reorganization and turnover of the actin cytoskeleton, we performed a scratch assay to measure VSMCs migration from WT and FPR-1 KO mice. As hypothesized, the migration was impaired in cells that did not express FPR-1 when compared to control (Figure 5 C and D).

Activation and stabilization of actin polymerization partially restored contraction in arteries from FPR-1 KO

Given that we observed that FPR-1 has an important role in vascular function (contraction and myogenic response) and this receptor triggers actin polymerization in VSMCs, we questioned if the loss of contraction observed in arteries from FPR-1 KO mice would be related to an impairment in actin polymerization. To answer this question, arteries were treated with jasplakinolide, an actin polymerization inducer, or cytochalasin D, an actin polymerization inhibitor. Interestingly, polymerization of F-actin with jasplakinolide improved contraction in all arteries studied from FPR-1 KO mice (Figure 6 D, E and F), but not in arteries from WT mice (Figure 6 A, B and C). On the other hand, depolymerization of F-actin using cytochalasin D, significantly decreased contraction in arteries from both FPR-1 KO and WT animals (Figure 6 G–L); however, the magnitude of this decrease was greater in WT animals (Figure 6 G, H and I).

Next, we investigated if Rho family GTPases play a role in vascular contraction via FPR-1 activation. Rho family GTPases regulate cytoskeletal dynamics, including stress fiber formation. Here, we observed that VSMC treated with non-formylated peptides or F-MIT (10 μM) induced phosphorylation of $MYPT1^{Thr696}$ (Figure 7 G), suggesting Rho-ROCK activation. As expected, we did not observe change in RhoA/ROCK protein expression (Figure 7 H and I) since RhoA-ROCK expression by itself does not regulate activity. Surprisingly, arteries treated with RhoA activator did not restore the impaired

phenylephrine-induced contraction observed in FPR-1 KO (Figure 7 D, E and F). We do not know why RhoA activator did not improved contraction in arteries from FPR-1 KO animals. However, given that RhoA-ROCK leads to actin polymerization in arteries, we could infer that the absence of contraction in the presence of RhoA activator is because actin polymerization is disrupted in arteries from FPR-1 KO.

Calcium homeostasis is impaired in arteries lacking FPR-1.

There is no doubt that an increase in cytosolic Ca^{2+} is the main mechanism to initiate arterial contraction and myogenic tone (Webb, 2003). Cytosolic Ca^{2+} is increased through Ca^{2+} release from intracellular stores (sarcoplasmic reticulum) as well as entry from the extracellular space through Ca^{2+} channels (voltage operated and receptor-operated Ca^{2+} channels) (Webb, 2003). Activation of FPR-1 also triggers an increase in cytosolic Ca^{2+} in neutrophils (Korchak *et al.*, 1998) Based on this evidence, we investigated if FPR-1 deletion would also decrease contraction via reduced Ca^{2+} influx. We did not observe differences in contraction induced by L-type calcium channel (Cav 1.2) activator, Bay K 8644 in aorta and resistance arteries (Figure 8 A, B and C) from WT and FPR-1 KO, suggesting that the Cav1.2-dependent Ca^{2+} influx is not impaired in arteries from FPR-1 KO. On the other hand, we found that the expression of Cav1.2 is significantly reduced in VSMC from FPR-1 KO (Figure 8 D), while no differences were observed between groups in PKCα protein expression (Figure 8 E).

To determine the changes in intracellular Ca^{2+} concentration in VSMC from WT and FPR-1 KO, we used a fluorescent indicator, fura-2-acetoxymethyl ester (fura-2 AM). Single-cell intracellular Ca^{2+} measurements on fura-2-loaded VSMC showed that baseline intracellular Ca^{2+} concentration (absence of stimulus) is higher in VSMC from FPR-1-KO when compared to WT. Addition of 120 mM of KCl led to a rapid and transient increase in the intracellular Ca^{2+} in both groups. However, this increase was significantly higher in FPR-1 KO VSMC when compared to WT (Figure 8 G. Table 1). Next, we wanted to know if the scaffolding protein Ahnak, also known as desmoyokin, could play a role in FPR-1 and Cav 1.2 function. Ahnak is a 700 kDa protein that has been implicated in essential biological functions such as cell migration and organization of the cell membrane cytoarchitecture, and that is critical for cardiac Cav 1.2 Ca^{2+} channel function (Haase *et al.*, 2005). Interestingly, Ahnak protein expression is ~50% reduced in VSMCs from FPR-1 KO (Figure 8 F).

Blood pressure measurements were similar between groups.

No differences were observed in basal arterial blood pressure (BP) (Mean BP: WT: 103 vs. FPR-1 KO: 104 mmHg, $p>0.05$) and heart rate (WT: 539 vs. FPR-1 KO: 563 bpm; $p>0.05$) between WT and FPR-1 KO animals. We infer that other mechanisms [e.g. increased vascular stiffness, as shown by the leftward shift in the stress-strain curve (Figure 4 A) and inward hypotrophic remodeling (Figure 4 F, G and H] would counterbalance the decreased contractility observed in arteries from FPR-1 KO mice. This would maintain normal blood pressure.

Discussion

Our observations revealed that the innate immune system pattern recognition receptor FPR-1 is also required for vascular homeostasis, including myogenic behavior during physiological conditions. Here, we have determined that the function of FPR-1 is not only limited to its detection of pathogens and DAMPs in the bloodstream, but it is also significant for the dynamic plasticity of the vasculature. We observed that upon activation (by agonist or stretch), FPR-1 plays a role in myogenic tone via an integrated network with actin cytoskeleton (Figure 9). Overall, these observations provide 1) a new mechanistic insight into how the immune and cardiovascular system form a network affecting vascular plasticity and 2) identify a mechanism by which interaction between cells of the immune system and arteries can mediate inter-tissue responses to danger.

Although N-formyl peptides are the main ligands for FPR-1, there are only two sources of these molecules in the human body, bacteria and mitochondria (Le *et al.*, 2001). Therefore, FPR-1 is fundamental for bacterial and mitochondrial clearance (Le *et al.*, 2001). The FPR family, a subfamily of G protein-coupled receptors, is represented by at least three isoforms, FPR 1, 2, and 3 (Le *et al.*, 2001; Wenceslau *et al.*, 2015;2016). Formyl peptide receptors are expressed at high levels in neutrophils and monocytes, and when activated by binding of FMLP (bacterial peptide) or F-MIT (mitochondrial peptide) (Wenceslau *et al.*, 2015;2016) they induce NADPH oxidase activation, ROS generation, and cell chemotaxis (Millar, 2016). Besides being expressed in neutrophils, the FPR family is expressed in a range of somatic cells and tissues, including the endothelium, epithelium, spleen, lung, liver, skeletal, and smooth muscle (Le *et al.*, 2001; Millar, 2016). Human FPR family receptors are intrinsically associated with the G_i protein subunit (Millar, 2016), and upon activation, FPR-1 triggers stimulation of phosphatidylinositol-3-kinase (PI3K), phospholipase C (PLC), protein kinase C (PKC), Ca^{2+} flux and mitogen-activated protein kinases (MAPKs) (Millar, 2016). Also, FPR-1 activation is important for wound healing mechanism (Millar, 2016), and is associated with neutrophil migration, via actin polymerization, to sites of sterile and non-sterile inflammation (McDonald *et al.*, 2010; Wenceslau et al., 2015;2016).

Because FPR-1 is expressed in VSMCs and its role in non-hematopoietic cells is still unclear, we questioned whether FPR-1 would have physiological relevance for vascular behavior, in the same way as it does in neutrophils (Ca^{2+} homeostasis and actin polymerization). First, we tested if FPR-1 is involved in arterial contraction. Indeed, here we observed that FPR-1 KO decreased acute and prolonged vascular contraction to receptor-dependent and -independent stimuli. Agonist-induced vasoconstriction in VSMCs has been attributed not only to a process in which receptor activation increase intracellular Ca^{2+} leading to myosin light-chain kinase activation and subsequent cycling of actin-myosin cross-bridges (acute contraction) in VSMCs, but recent evidence demonstrated that prolonged contraction is related to actin polymerization (Staiculescu *et al.*, 2013) Accordingly, Dr. Martinez-Lemus's group (2013) has shown that exposure of isolated arterioles to vasoconstrictor agonists induces VSMCs actin polymerization via activation of small GTPases (Staiculescu *et al.*, 2013). Also, several studies support the conclusion that VSMC contraction is accompanied by an increase in F-actin and a decrease in G-actin content (Walsh & Cole, 2013). Measurements of F- and G-actin ratio at rest and after

stimulation by using adrenergic receptors (in vessels) or muscarinic receptors (in airways) agonists demonstrated that cellular actin undergoes polymerization (Walsh & Cole, 2013). Drs. Walsh and Cole (2013) described that this response is consistent with the presence of two pools of cellular actin: one (‘contractile actin’) involved in the contractile machinery, associated with tropomyosin and stabilized in the filamentous form, and the other (‘cytoskeletal actin’) localized to the cell cortex, not associated with tropomyosin and undergoing reversible polymerization–depolymerization (Walsh & Cole, 2013). In the present study, we found that the direct activation of actin polymerization ameliorates contractility in arteries from FPR-1 KO. This result revealed that FPR-1 is essential for sustained contraction via actin polymerization. To further confirm that FPR-1 plays a role in actin polymerization in VSMCs, we observed that FPR-1 agonist, mitochondrial N-formyl peptides (F-MIT), increased F:G actin ratio, and specific FPR-1 inhibitors abolished this result. Supporting these findings, using confocal microscopy we demonstrated that F-actin bundles were disorganized in VSMCs from FPR-1 KO mice when compared to control. Another piece of supporting evidence that FPR-1 indeed plays a role in smooth muscle cell (SMC) contractility was seen in our previous study (Wenceslau *et al.*, 2016), where FPR activation leads to trachea, bronchus and bronchiole (no endothelial cell influence) contractile responses and activate cell division control protein 42 (CDC42). Actin cytoskeletal remodeling is an important component of airway smooth muscle contraction (Kim *et al.*, 2011). Up-regulation of a cytoskeletal recruitment in highly shortened airway smooth muscle has been shown to be an important mechanism of reduced airway distensibility (Kim *et al.*, 2011). Also, CDC42 is a member of Rho GTPase family, which regulates F-actin reorganization and induces actin polymerization, either by stimulating *de novo* actin nucleation or by stimulating the uncapping or severing of filaments (Macheskya *et al.*, 1999). Additionally, in a previous publication we observed that lipoxin A_4 (an endogenous FPR agonist) induces acute and prolonged contraction in aorta from naïve animals. The contractions were abolished in the presence of Y27631 (RhoA/Rho kinase inhibitor). Therefore, these studies confirm our hypothesis that FPR plays a role in SMC contractility (acute and chronic), independent of developmental changes. In the present study, we observed that sustained vasoconstriction and actin polymerization via FPR-1 could also be via small GTPases, including RhoA/ROCK, given that VSMCs treated with FPR agonist induced MYPT1 phosphorylation. However, RhoA activator did not improve contraction in arteries from FPR-1 KO, this could be due to the presence of disruption of actin polymerization.

Actin polymerization is crucial for cell migration, and cell migration is a critical response in vascular homeostasis. Our experiments revealed that migration is diminished in VSMCs from FPR-1 KO. We did not investigate the mechanism of how FPR-1 induces migration, but it seems plausible that FPR-1-induced actin polymerization would be implicated.

As described above, Ca^{2+} signaling is critical for vascular contraction and, upon activation, FPR-1 triggers Ca^{2+} increase in neutrophils, which subsequently leads to migration, ROS generation and cytokines release (Le *et al.*, 2001; Millar, 2016). Given the importance of Ca^{2+} influx to vascular contraction, we performed a concentration-response curve to Cav 1.2 activator, Bay K 8644. We did not observe differences in contraction induced by this compound in resistance arteries and aorta from WT and FPR-1 KO, suggesting that the

Cav1.2-dependent Ca^{2+} influx is not impaired in arteries from FPR-1 KO. Also, we used a fluorescent indicator, fura-2-acetoxymethyl ester (fura-2 AM) to measure intracellular Ca^{2+} in VSMC in the presence or absence of FPR-1. Single-cell intracellular Ca^{2+} measurements on fura-2-loaded VSMC showed that baseline intracellular Ca^{2+} concentrations (absence of stimulus) is higher in VSMC from FPR-1-KO when compared to WT. Addition of 120 mM of KCl led to a rapid and transient increase in the intracellular Ca^{2+} in both groups. This increase was significantly higher in VSMC from FPR-1 KO when compared to WT. These data discard the fact that reduction of intracellular Ca^{2+} would be the main factor that leads to decreased contraction in FPR-1 KO arteries. Actually, it was the opposite then the expected, intracellular concentration of Ca^{2+} was higher in cells from FPR-1 KO. This could be a compensatory mechanism due to decrease of L-type Ca^{2+} (Cav1.2) expression. We do not know why Cav1.2 expression is decreased in FPR-1 KO, but it is possible to speculate that there is an interaction between FPR-1 and Cav1.2, or maybe a possible transactivation. We suggested that a possible link between FPR-1 and Cav 1.2. is a 700 kDa scaffolding protein called Ahnak. Recent evidence has demonstrated that this protein interacts directly with Cav 1.2. and this interaction is important for proper cardiac function (Haase *et al.*, 2005). Furthermore, it has been reported that Ahnak provides a structural basis for the subsarcolemmal cytoarchitecture and confers the regulatory role of the actin-based cytoskeleton to the L-type Ca^{2+} channel (Hohaus *et al.*, 2002), which means that Ahnak could directly influence actin polymerization and Cav 1.2. function. To further support our hypothesis that Ahnak could form a complex with FPR-1 and Cav 1.2, a recent study showed that Ahnak interacts with the annexin 2/S100A10 complex, and it is well known that annexin I receptors belong to FPR family (Walther *et al.*, 2000). Here, we demonstrated that loss of FPR-1 leads to significant reduction of Ahnak protein expression. Therefore, based on this result we can infer that Cav 1.2 is connected to FPR-1 via Ahnak, which could interact with cytoskeleton leading to actin polymerization and, subsequently this complex modulates contractility. However, this result is too preliminary and needs further investigation.

As demonstrated by Bayliss in 1902, myogenic response is the ability of the blood vessels to contract in response to intraluminal pressure elevation. This is intrinsic to VSMCs, particularly in small arteries (dimeter < 200 μm), and this response is triggered by stretch. The vascular wall receptor sites and the transduction pathways for this phenomenon are not completely understood; however, these are believed to be related to stretch-induced opening of cell-membrane Ca^{2+} channels (Meininger & Davis, 1992). Recently, actin polymerization within VSMCs in response to increased intravascular pressure was recognized as a novel mechanism underlying arterial myogenic mechanism (Cipolla *et al.*, 2002). Interestingly, it has been shown that undifferentiated human promyelocytic leukemia cells (HL60) that lacked FPR do not respond to shear stress, whereas expression of FPR in undifferentiated HL60 cells caused pseudopod projection and robust pseudopod retraction during fluid shear (Makino *et al.*, 2006). These results suggested that FPR-1 could serve as mechanosensor for fluid shear stress (Makino *et al.*, 2006). Because of this evidence, we subsequently postulated that FPR-1 would act as a mechanosensing like-receptor in arteries. Therefore, this receptor would be able to sense changes in pressure and be implicated in the myogenic response. Indeed, in the present study we demonstrated that pressure-induced myogenic

response is lost in arteries lacking FPR-1. We suggested that FPR-1 acts as a mechansensor via the network it forms with actin filaments, and this then affects the myogenic response via actin polymerization. Not all GPCRs are necessarily a mechanical sensor. FPR has been implicated as a sensor for fluid shear stress, but other chemoattractant GPCRs, such as CXCR1 and CXCR2, did not display unique properties while exposed to shear stress (Mitchell *et al.* 2012). Although we do not know at present why FPR-1 receptor is significantly activated by mechanical stretch, there are a few possibilities. First, differences in its response to fluid shear stress could involve differences in its signaling pathways, as neutrophil chemotaxis in response to either FMLP (FPR agonist) or IL-8 is known to display different properties. Second, diversity in the structures and expression of the receptors may also determine their responsibility to mechanical stress. It is very interesting that a decrease in FPR-1 surface expression in neutrophils, due to internalization, is direct associated with reduction of pseudopods formation (Mitchell *et al.* 2012), which is well known to be linked to actin polymerization. Therefore, we have confidence that FPR indeed contributes to the mechanosensing responses of cells within the vascular microenvironment, similar to observed in neutrophils.

A similar concept was observed when AT1 receptor was recognized as a mechanosensor. In line, Zou et al. (2004) demonstrated that although not all GPCRs were activated by stretch in the heart, AT1R was. They observed that mechanical stretch induced a conformational change in the AT1R and subsequently association with Janus kinase 2, and translocation of G proteins into the cytosol. Also, studies with PKC inhibitors have suggested a role for this kinase in the myogenic response of resistance arteries, but the underlying mechanism remains unclear (Moreno-Domínguez *et al.*, 2013). Accordingly, it has been shown that the PKC inhibitors suppressed the myogenic response of rat middle cerebral arteries (Walsh & Cole, 2013). Because agonists for FPR lead to PKC activation, we wanted to understand if FPR-1 absence would change PKC expression. We did not observed differences in expression for this protein between WT and FPR-1 KO. However, further studies are necessary to understand if the activity of this kinase is altered by FPR-1 absence/activation. Since it has been observed that Ca^{2+} sensitization via phosphorylation of myosin phosphatase targeting subunit at threonine-855 by Rho kinase contributes to the arterial myogenic response (Johnson et al., 2009), another possible mechanism that could be associated with FPR-1 and myogenic tone would be RhoA/ROCK activation. Here, we observed that FPR-1 activation induced MYPT1 phosphorylation (Figure 7G), but additional experiments needs to be performed to support this hypothesis.

According to Laplace's law, loss of myogenic response would increase wall stress and tension in downstream vessels and subsequently induce endothelial dysfunction and arterial stiffness (Holmberg *et al.,* 2018). Indeed, we found that arteries from FPR-1 KO mice presented with a leftward shift in the stress-strain curve and decreased distensibility, suggesting that these arteries are stiffer in basal conditions. One important concept of vascular mechanics is that proportional composition of blood vessels influences passive distensibility of the vessel wall. The concept considers the relation between structure and mechanics of the vessel wall in terms of the elastic moduli of individual wall components (Baumbach *et al.* 1991). In an interesting study, Baumbach *et al.* (1991) showed that in hypertension one mechanism that may protect cerebral vessels is increases in passive

distensibility of cerebral arterioles. They suggested that increases in passive distensibility of cerebral arterioles, therefore, may increase effectiveness of autoregulation of cerebral blood flow in SHRSP. Likewise, in the present manuscript, we observed that arteries from FPR-1 KO animals presented decreased in distensibility and myogenic tone when compared to WT. This suggests that impairments in distensibility would lead to damage of myogenic tone and, subsequently a stiffer artery.

As described above, we also found that arteries of FPR-1 KO exhibit reduction in the internal and external diameter and, consequently, a reduction in cross-sectional area (CSA) which suggests an inward hypotrophic remodeling. It is known that circumferencial wall stress and wall shear stress are important driving forces during development of the arterial wall and in the adult (Rubanyi et al., 1990; Pourageaud & De Mey, 1997). Vascular remodeling can result in either an increase, no change, or a decrease in the amount of material, that there should be a sub-classification into hypertrophic, eutrophic, and hypotrophic remodeling, respectively (Mulvany 1999). Only few studies were able to observe inward hypotrophic remodeling (Pourageaud and Mey, 1997). Accordingly, it is known that reduced blood flow results in inward hypotrophic remodeling accompanied by hyporeactivity of the arterial smooth muscle (Pourageaud and Mey, 1997). In the present manuscript, we also observed hyporeactivity to adrenergic receptor agonist, however a causative relationship between inward hypotrophic remodeling, blood flow and hyporeactivity was not assessed in the present study, and will be the subject of future studies.

Overall, our results reveal a unique function for FPR-1 in mediating vascular plasticity during physiological conditions. Upon activation (by agonist or stretch), FPR-1 triggers actin polymerization by mechanisms that are still unclear (Figure 9). However, based on preliminary data we could infer that FPR-1 may act via an integrated network with Cav 1.2, RhoA, and actin polymerization. Future studies are needed to dissect the mechanisms associated with FPR-1 activation and its functions as a mechanosensor-like receptor and vascular-immuno network during perturbations.

Acknowledgements

We would like to thank Vadym Buncha and Alena Cherezova for their excellent technical expertise.

Funding

This work was supported by National Institutes of Health (NIGMS: K99GM11888 – **C.F.W.**; and NHLBI: P01 P01HL134604 - **R.C.W.**)and American Heart Association (18POST34060003 – **C.G.M.**)

Abbreviations:

FPR	formyl peptide receptor
VSMCs	vascular smooth muscle cells
Cav 1.2	L-type calcium channels
DAMPS	damage-associated molecular patterns
F-MIT	mitochondrial formylated peptides

JASP	jasplakinolide
MRA	mesenteric resistance arteries
PKC	protein kinase C
Ahnak	Neuroblast differentiation-associated protein
wild-type	WT
CsH	cyclosporine H
CYTO	cytochalasin B
CdC42	cell division control protein 42 homolog
CSA	cross-sectional area

References

1. Ananthakrishnan R & Ehrlicher A (2007). The Forces Behind Cell Movement. Int J Biol Sci 3, 303–317. [PubMed: 17589565]
2. Baumbach GL, Siems JE, Heistad DD (1991). Effects of local reduction in pressure on distensibility and composition of cerebral arterioles. Circ Res 68, 338–51. [PubMed: 1991342]
3. Bayliss WM (1902). On the local reactions of the arterial wall to changes of internal pressure. J. Physiol. Lond 28, 220–231. [PubMed: 16992618]
4. Briones AM, Salaices M, Vila E (2007). Mechanisms underlying hypertrophic remodeling and increased stiffness of mesenteric resistance arteries from aged rats. J Gerontol A Biol Sci Med Sci 62, 696–706. [PubMed: 17634315]
5. Cipolla MJ, Gokina NI, Osol G (2002). Pressure-induced actin polymerization in vascular smooth muscle as a mechanism underlying myogenic behavior. FASEB J 16, 72–76. [PubMed: 11772938]
6. Grundy D (2015). Principles and standards for reporting animal experiments in The Journal of Physiology and Experimental Physiology. J Physiol 593, 2547–2549. [PubMed: 26095019]
7. Haase H, Alvarez J, Petzhold., Doller A, Behlke J, Erdmann J, Hetzer R, Regitz-Zagrosek V, Vassort G, Morano I (2005). Ahnak is critical for cardiac Ca(V)1.2 calcium channel function and its beta-adrenergic regulation. FASEB J 19, 1969–19677. [PubMed: 16319140]
8. Hohaus A, Person V, Behlke J, Schaper J, Morano I, Haase H (2002). The carboxyl-terminal region of ahnak provides a link between cardiac L-type Ca2+ channels and the actin-based cytoskeleton. FASEB J 16, 1205–1216. [PubMed: 12153988]
9. Holmberg J, Bhattachariya A, Alajbegovic A, Rippe C, Ekman M, Dahan D, Hien T, Boettger T, Braun T, Swärd K, Hellstrand P, Albinsson S (2018). Loss of Vascular Myogenic Tone in miR-143/145 Knockout Mice Is Associated With Hypertension-Induced Vascular Lesions in Small Mesenteric Arteries. Arterioscler Thromb Vasc Biol 38, 414–424. [PubMed: 29217510]
10. Johnson RP, El-Yazbi AF,1 Takeya K, Walsh EJ, Walsh MP, Cole WC. Ca2+ sensitization via phosphorylation of myosin phosphatase targeting subunit at threonine-855 by Rho kinase contributes to the arterial myogenic response. J Physiol. 2009 6 1; 587(Pt 11): 2537–2553. [PubMed: 19359365]
11. Kim HR, Liu K, Roberts TJ, Hai CM (2011). Length-dependent modulation of cytoskeletal remodeling and mechanical energetics in airway smooth muscle. Am J Respir Cell Mol Biol 44, 888–897. [PubMed: 20705939]
12. Korchak HM, Vosshall LB, Zagon G, Ljubich P, Rich AM, Weissmann G (1998). Activation of the neutrophil by calcium-mobilizing ligands. I. A chemotactic peptide and the lectin concanavalin A stimulate superoxide anion generation but elicit different calcium movements and phosphoinositide remodeling. J Biol Chem 263, 11090–11097.

13. Le Y, Murphy PM, Wang JM (2001). Formyl-peptide receptors revisited. Trends Immunol 23, 541–8.
14. Macheskya LM, Insalla RH (1999). Signaling to actin dynamics. J. Cell Biol 146, 267–272. [PubMed: 10427083]
15. Makino A, Prossnitz ER, Bünemann M, Wang JM, Yao W, Schmid-Schönbein GW (2006). G protein-coupled receptors serve as mechanosensors for fluid shear stress in neutrophils. Am J Physiol Cell Physiol 290, C1633–1639. [PubMed: 16436471]
16. McCarthy CG, Wenceslau CF, Ogbi S, Szasz T, Webb RC (2018). Toll-like receptor 9-dependent AMPKα activation occurs via TAK1 and contributes to RhoA/ROCK signaling and actin polymerization in vascular smooth muscle cells. J Pharmacol Exp Ther 365(1), 60–71. [PubMed: 29348267]
17. McDonald B, Pittman K, Menezes GB, Hirota SA, Slaba I, Waterhouse CC, Beck PL, Muruve DA, Kubes P (2010). Intravascular danger signals guide neutrophils to sites of sterile inflammation. Science. 330, 362–366. [PubMed: 20947763]
18. Meininger GA & Davis MJ (1992). Cellular mechanisms involved in the vascular myogenic response. Am J Physiol 263, H647–59. [PubMed: 1415587]
19. Millar BJM (2016). The role of the formyl-peptide receptor in multi-organ fibrosis mechanisms. Newcastle University. Thesis [http://hdl.handle.net/10443/3500].
20. Mitchell MJ, King MR (2012). Shear-induced resistance to neutrophil activation via the formyl peptide receptor. Biophys J 102, 1804–14. [PubMed: 22768936]
21. Moazzam F, DeLano FA, Zweifach BW, Schmid-Schönbein GW (1997). The leukocyte response to fluid stress. PNAS 94, 5338–5343. [PubMed: 9144238]
22. Moreno-Domínguez A, Colinas O, El-Yazbi A, Walsh EJ, Hill MA, Walsh MP, Cole WC (2013). Ca2+ sensitization due to myosin light chain phosphatase inhibition and cytoskeletal reorganization in the myogenic response of skeletal muscle resistance arteries. J Physio 591, 1235–1250
23. Mulvany MJ, Halpern W (1977). Contractile properties of small arterial resistance vessels in spontaneously hypertensive and normotensive rats. Circ Res 41, 19–26. [PubMed: 862138]
24. Mulvany MJ (1999). Vascular remodelling of resistance vessels: can we define this? Cardiovascular Research, 41, 9–13. [PubMed: 10325946]
25. Nakamura M, Sunagawa M, Kosugi, Sperelakis N (2000). Actin filament disruption inhibits L-type Ca(2+) channel current in cultured vascular smooth muscle cells. Am J Physiol Cell Physiol 279, C480–487. [PubMed: 10913014]
26. Norgauer J, Krutmann J, Dobos GJ, Traynor-Kaplan AE, Oades ZG, Schraufstätter IU (1994). Actin polymerization, calcium-transients, and phospholipid metabolism in human neutrophils after stimulation with interleukin-8 and N-formyl peptide. J Invest Dermatol 102, 310–4. [PubMed: 8120414]
27. Pourageaud F and De Mey JGR (1997). Structural properties of rat mesenteric small arteries after 4-wk exposure to elevated or reduced blood flow. Am. J. Physiol - Heart Circ. Physiol 273, H1699–H1706.
28. Prasain N, Stevens T (2009). The actin cytoskeleton in endothelial cell phenotypes. Microvasc Res 77, 53–63. [PubMed: 19028505]
29. Rembold CM, Tejani AD, Ripley ML, Han S (2007). Paxillin phosphorylation, actin polymerization, noise temperature, and the sustained phase of swine carotid artery contraction. Am J Physiol Cell Physiol 293, C993–C1002. [PubMed: 17596300]
30. Rubanyi GM, Freany AD, Kauser K, Johns A, and Harder DR (1990). Mechanoreception by the endothelium: mediators and mechanisms of pressure- and flow-induced vascular response. Blood Vessels 27, 246–257. [PubMed: 2242445]
31. Staiculescu MC, Galiñanes E, Zhao G, Ulloa U, Jin M, Beig MI, Meininger GA., Martinez-Lemus LA (2013). Prolonged vasoconstriction of resistance arteries involves vascular smooth muscle actin polymerization leading to inward remodeling. Cardiovasc Res 98, 428–36. [PubMed: 23417038]
32. Storm DS, Webb RC (1993). Contractile Responses to Bay K 8644 in Rats with Coarctation-Induced Hypertension. Proc Soc Exp Biol Med 203, 92–99. [PubMed: 7682719]

33. Walther A, Riehemann K, Gerke V (2000). A novel ligand of the formyl peptide receptor: annexin I regulates neutrophil extravasation by interacting with the FPR. Mol Cell 5, 831–40. [PubMed: 10882119]
34. Walsh MP & Cole WC. The Role of Actin Filament Dynamics in the Myogenic Response of Cerebral Resistance Arteries (2013). J Cereb Blood Flow Metab 33, 1–12. [PubMed: 23072746]
35. Webb RC (2003). Smooth muscle contraction and relaxation. Adv Physiol Educ 27, 201–6. [PubMed: 14627618]
36. Wenceslau CF, McCarthy CG, Szasz T, Goulopoulou S, Webb RC (2015). Mitochondrial N-formyl peptides induce cardiovascular collapse and sepsis-like syndrome. Am J Physiol Heart Circ Physiol 308(7), H768–77. [PubMed: 25637548]
37. Wenceslau CF, Szasz T, McCarthy CG, Baban B, NeSmith E, Webb RC (2016). Mitochondrial N-formyl peptides cause airway contraction and lung neutrophil infiltration via formyl peptide receptor activation. Pulm Pharmacol Ther 37, 49–56. [PubMed: 26923940]
38. Wenceslau CF, Rossoni LV (2014). Rostafuroxin ameliorates endothelial dysfunction and oxidative stress in resistance arteries from deoxycorticosterone acetate-salt hypertensive rats: the role of Na +K+-ATPase/cSRC pathway. J Hypertens 32, 542–54. [PubMed: 24309491]
39. Yamin R & Morgan KG (2012). Deciphering actin cytoskeletal function in the contractile vascular smooth muscle cell. J Physiol 590, 4145–4154. [PubMed: 22687615]
40. Zou Y, Akazawa H, Qin Y, Sano M, Takano H, Minamino T, Makita N, Iwanaga K, Zhu W, Kudoh S, Toko H, Tamura K, Kihara M, Nagai T, Fukamizu A, Umemura S, Iiri T, Fujita T & Komuro I (2004). Mechanical stress activates angiotensin II type 1 receptor without the involvement of angiotensin II. Nat Cell Biol 6, 499–506. [PubMed: 15146194]

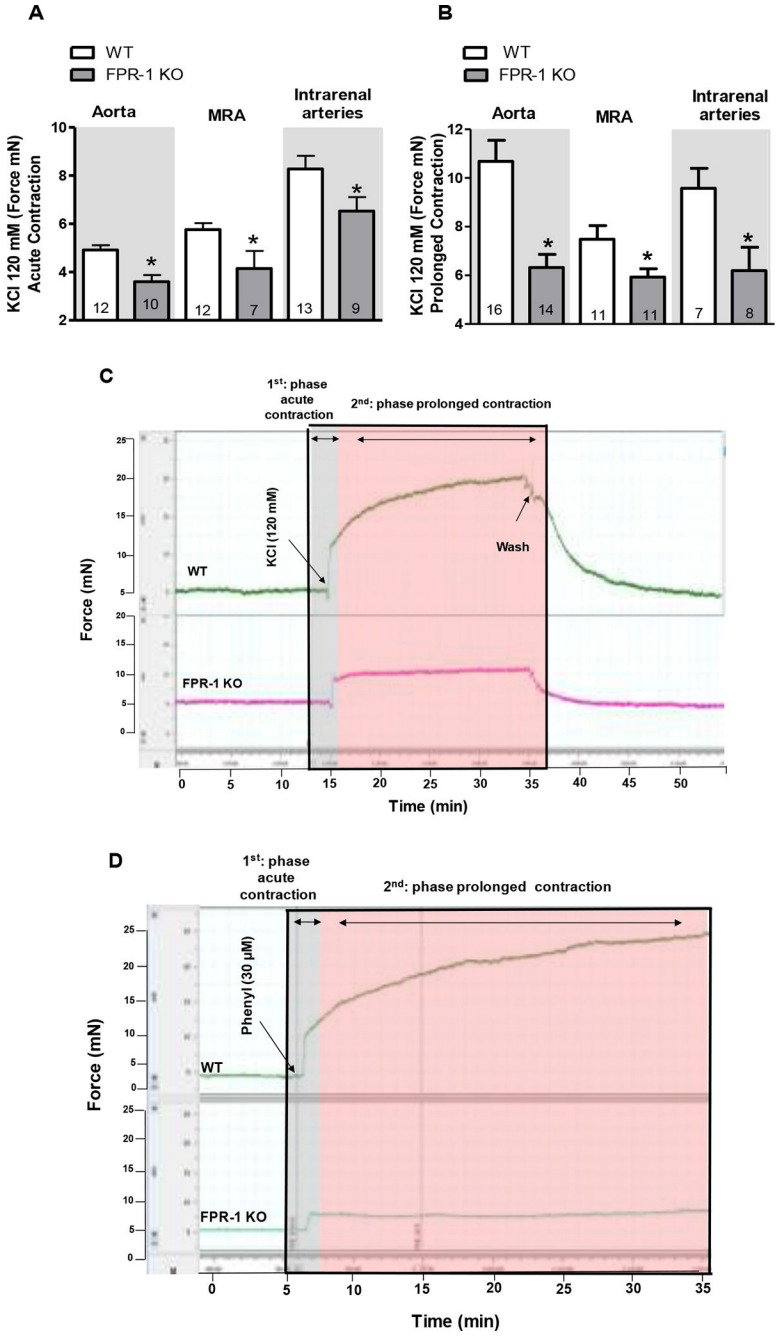

Figure 1.

Absence of FPR-1 decreases both acute (seconds-minutes) and prolonged (minutes-hours) contraction in aorta, mesenteric resistance arteries (MRA) and intrarenal arteries (A and B). Bar graphs show KCl-induced acute (A) and prolonged (B) contraction (120 mM). Typical traces represent KCl-(C) or phenylephrine-(D) induced contraction in aorta. Number (n) of the animals used is indicated in the graphs. Student's t-test or two-way ANOVA: *$p<0.05$ vs. wild-type (WT).

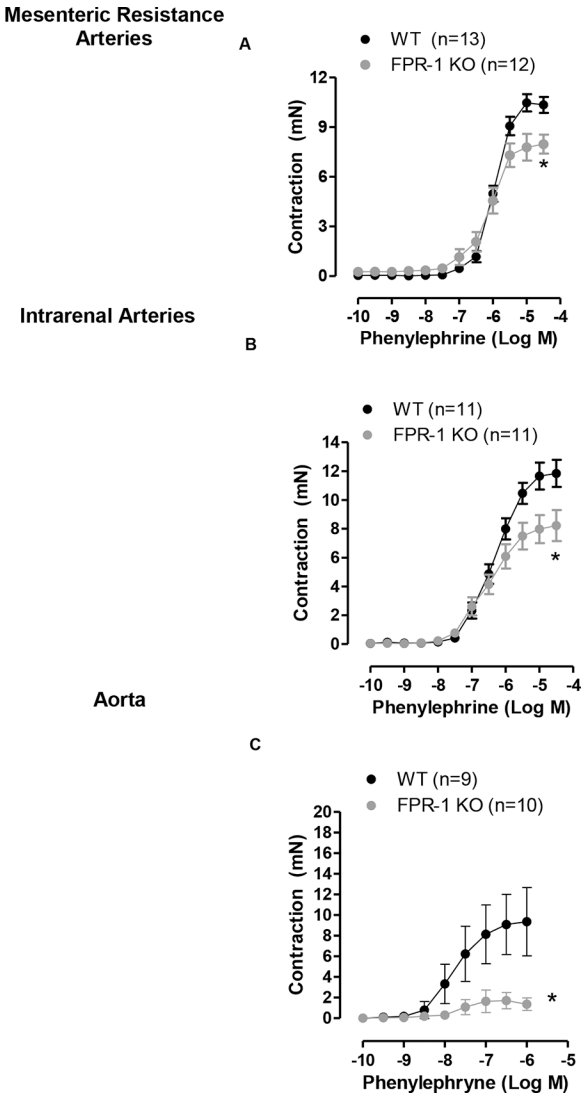

Figure 2:

Concentration response-curves to phenylephrine in mesenteric resistance arteries (A), intrarenal arteries (B) and aorta (C) from wild-type (WT) or FPR-1 KO mice. Number (n) of the animals used is indicated in the graphs. Two-way ANOVA: *p<0.05 vs. WT.

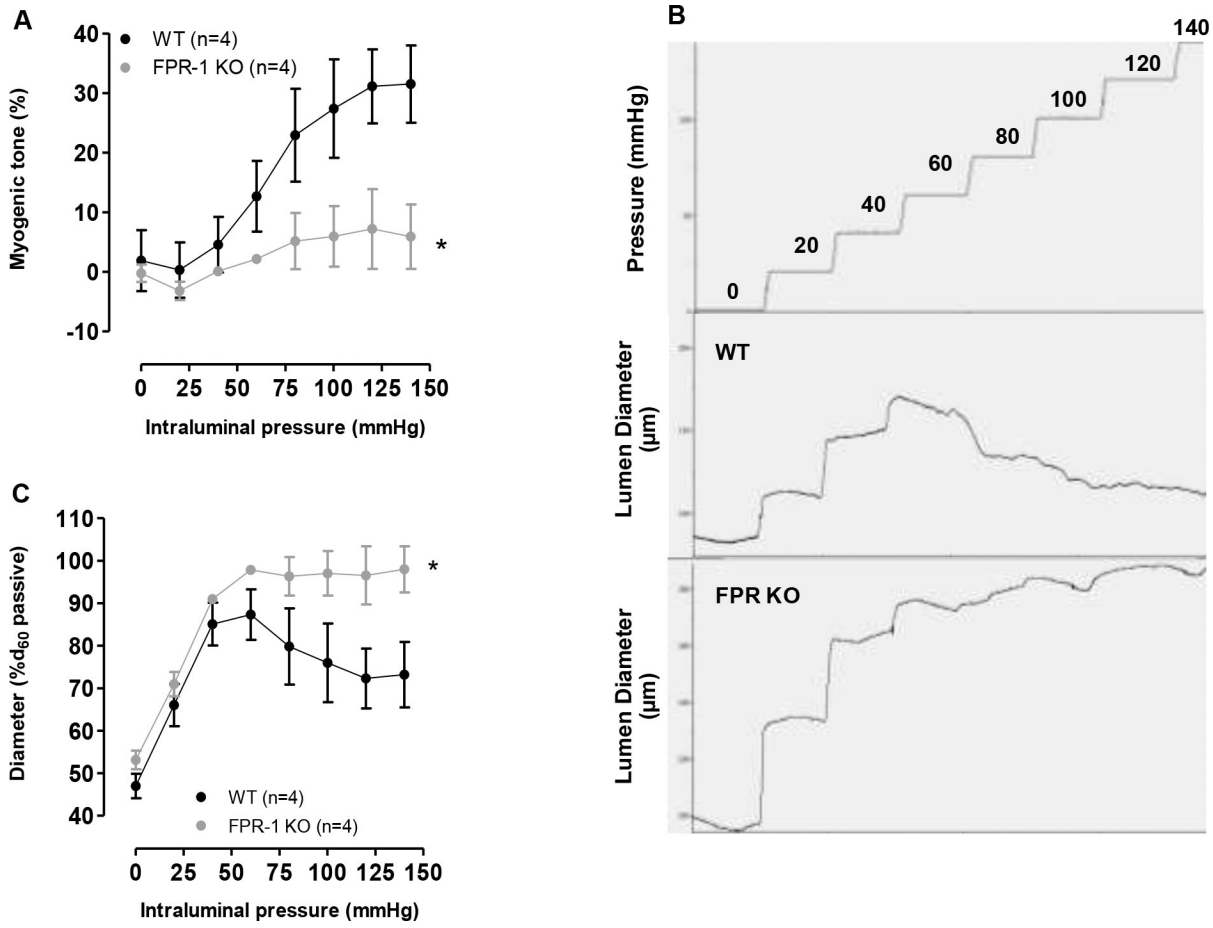

Figure 3.

Pressure-induced myogenic responses are lost in mesenteric resistance arteries (MRA) lacking FPR-1 (FPR-1 KO) when compared to wild-type (WT) mice (A). Typical trace for incremental increases in intraluminal pressure (mmHg) and changes in the lumen diameter (μm) in MRA (B). Diameters observed at each pressure were normalized to passive diameter at 60 mmHg (%d60passive) (C). Number (n) of the animals used is indicated in the graphs. Student's t-test or two-way ANOVA: *$p<0.05$ vs. wild-type (WT).

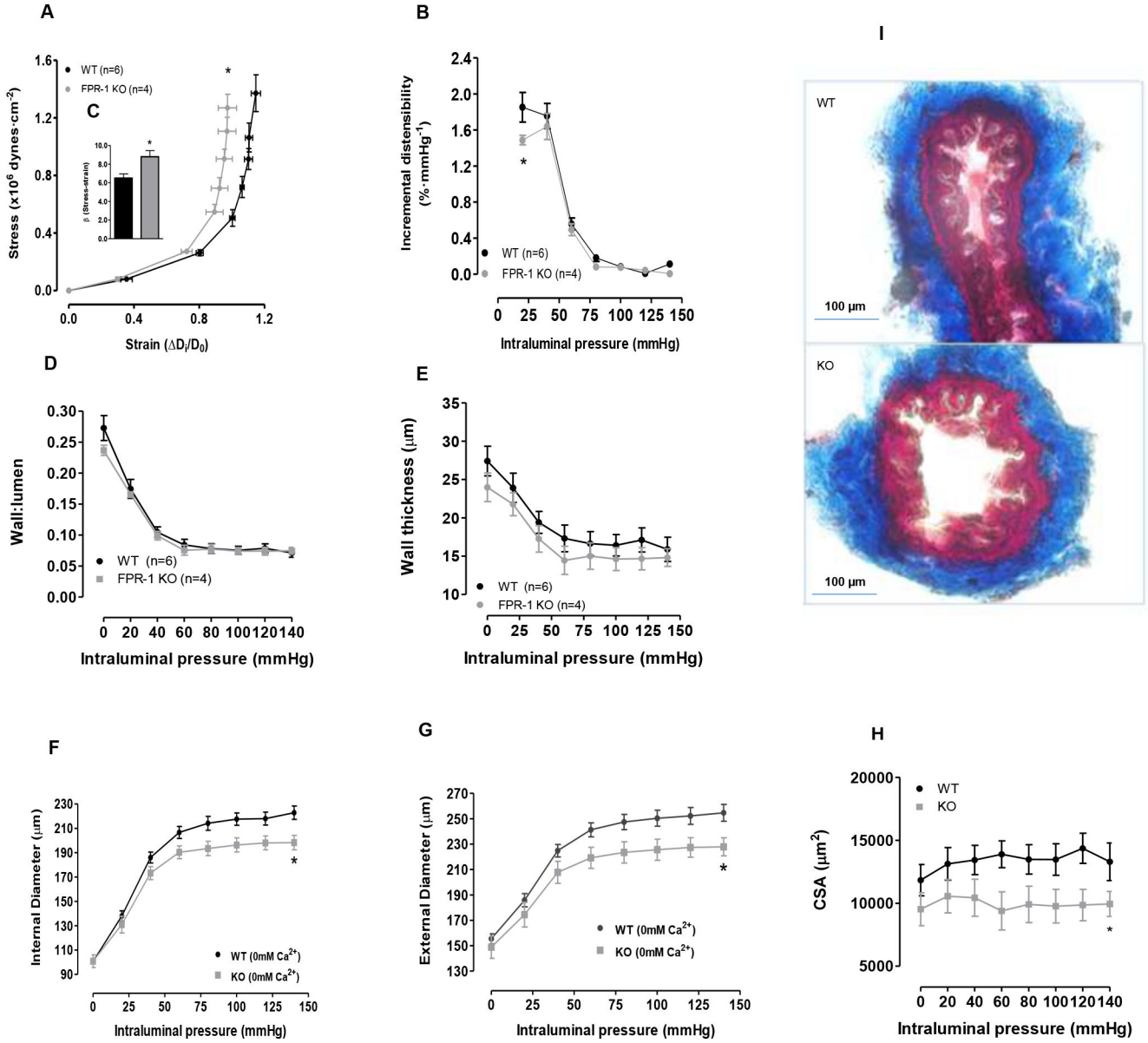

Figure 4:

Graphs: Stress-strain curves (A). Incremental distensibility (B) represents the percentage of change in the MRA internal diameter for each mmHg change in intraluminal pressure. β-values (slopes of the stress-strain relationships) (C). Wall:lumen ratio ($D_{e0Ca} - D_{i0Ca}$)/ $2D_{i0Ca}$) (D) and wall thickness (E) ((De0Ca − Di0Ca)/2) were measured during incremental in intraluminal pressure (mmHg) in mesenteric resistance arteries from wild-type (WT) and FPR-1 KO mice. Internal (F) and external diameter–intraluminal pressure (G), and cross-sectional area (CSA) (H). Masson's trichrome staining of collagen (I) in meseteric resistance arteries. Two-way ANOVA: *p<0.05.

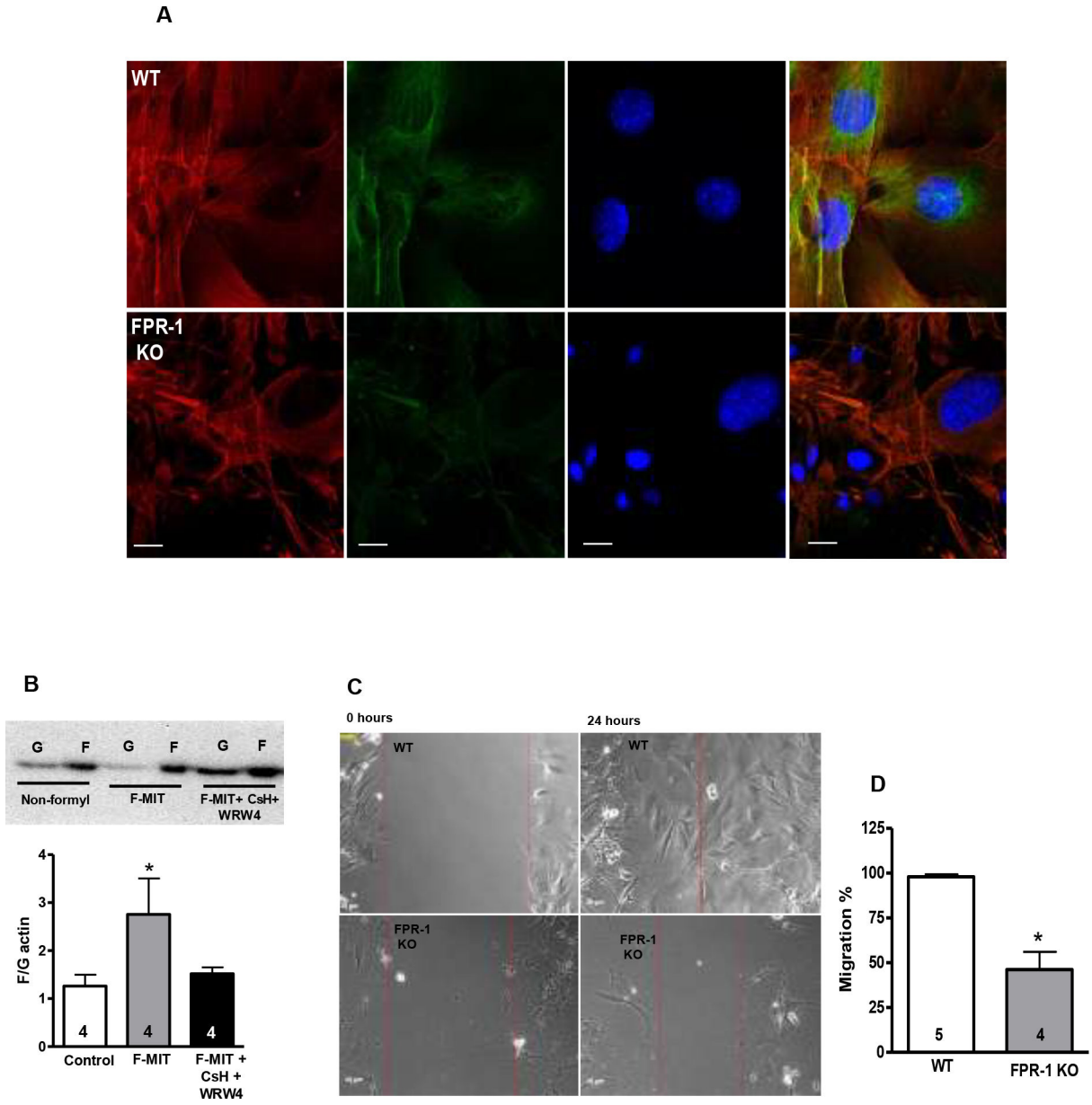

Figure 5.

Confocal microscopy (63X objective) (A) was performed to observe F-actin accumulation and organization (red), as well as immunofluorescence of α-tubulin (green) and nucleus (blue) in vascular smooth muscle cells (VSMCs) from wild-type (WT) or FPR-1 KO mice. FPR-1 agonist (mitochondrial N-formyl peptides, F-MIT, (20 min, 10 μM) increased filamentous F-to-globular G-actin ratio in VSMCs (B) from naïve animals. FPR-1 antagonists [cyclosporine H (CsH), 1 μmol/L or WRW4, 10 μmol/L, 30 min] reversed this response (B). Non formylated peptides (non-formyl) were used as control (B). Above, representative images of immunoblots; below, densitometric analysis (B). Scratch or wound healing assay in VSMCs from WT or FPR-1 KO showing migration after 24 h of the scratch (C and D). Number (n) of the animals used is indicated in the graphs. Student's t-test or one-way ANOVA: *p<0.05 vs. WT.

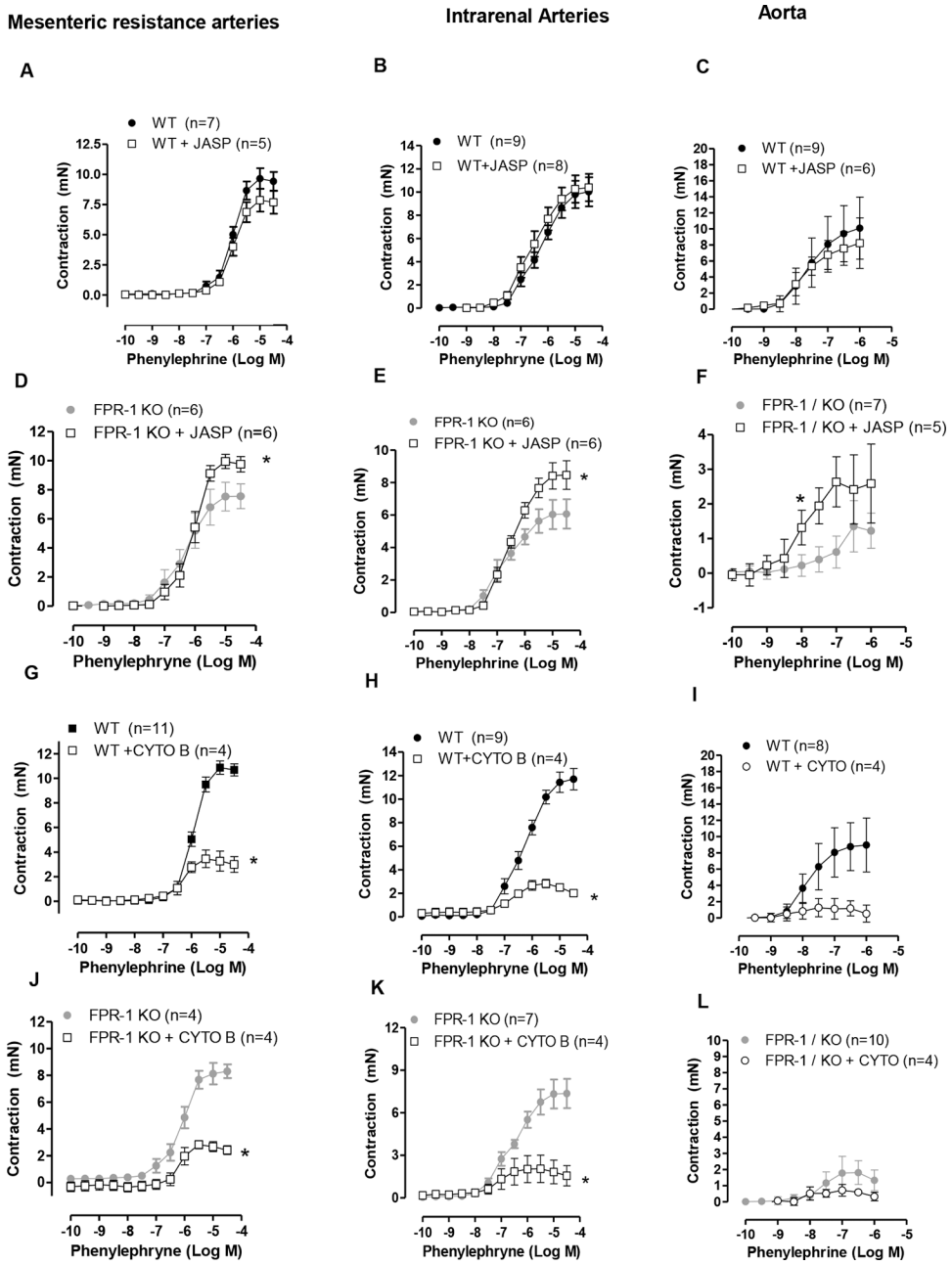

Figure 6.

Actin polymerization activator jasplakinolide (JASP, 0.1 μmol/l, 45 min) did not change phenylephrine-induced contraction in arteries from wild-type animals (WT, A, B and C). However, this factor increased contraction in arteries from FPR-1 KO mice (D, E and F). Actin polymerization inhibitor, cytochalasin B (CYTO, 1 μmol/l, 45 min) decreased phenylephrine-induced contraction in arteries from WT and FPR-KO mice (G-L). Number (n) of the animals used is indicated in the graphs. Two-way ANOVA, $p<0.05$, *vs WT (absence of CYTO); or *vs. FPR-1 KO (absence of JASP).

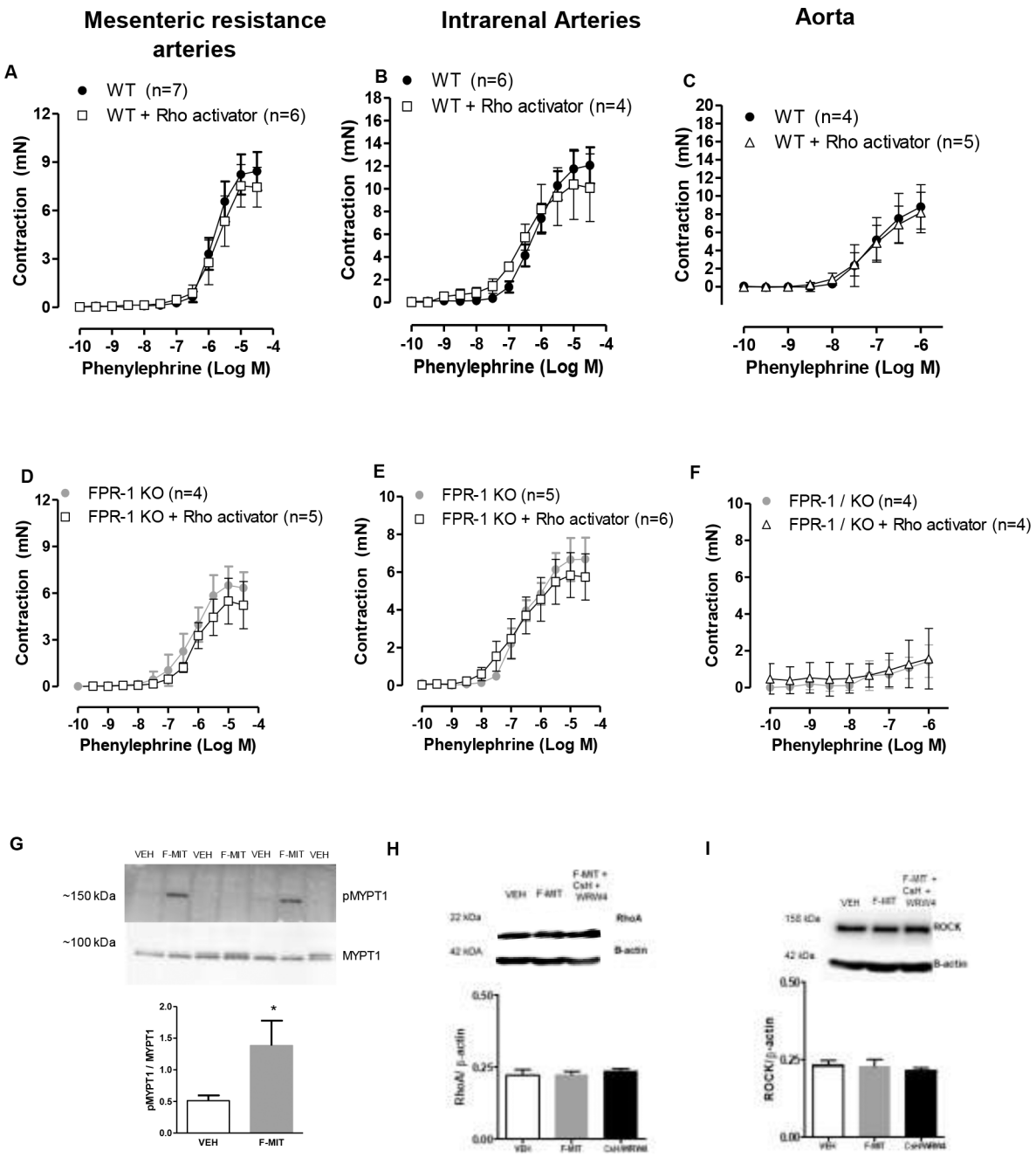

Figure 7.

RhoA activator (1.25 μg/ml, 2 hours) did not change concentration-response curves to phenylephrine in arteries from wild-type (WT; A, B and C) or FPR-1 KO mice (D, E and F). Two-way ANOVA, $p>0.05$. Western blot was used to investigate if FPR-1 activation induces changes in RhoA/ROCK and MYPT1 signaling protein expression. VSMCs were treated with F-MIT (20 min, 10 μM) in the presence or absence of a cocktail of FPR antagonists (cyclosporine H: CsH 1 μmol/l and WRW4 10 μmol/l, 30 min). Protein expression of pMYPT1Thr696 and MYPT1 (G), RhoA (H) or Rho-associated kinase (Rhokinase/ROCK) (I). Number (n) of the animals used is indicated in the graphs. One-way ANOVA, $p>0.05$.

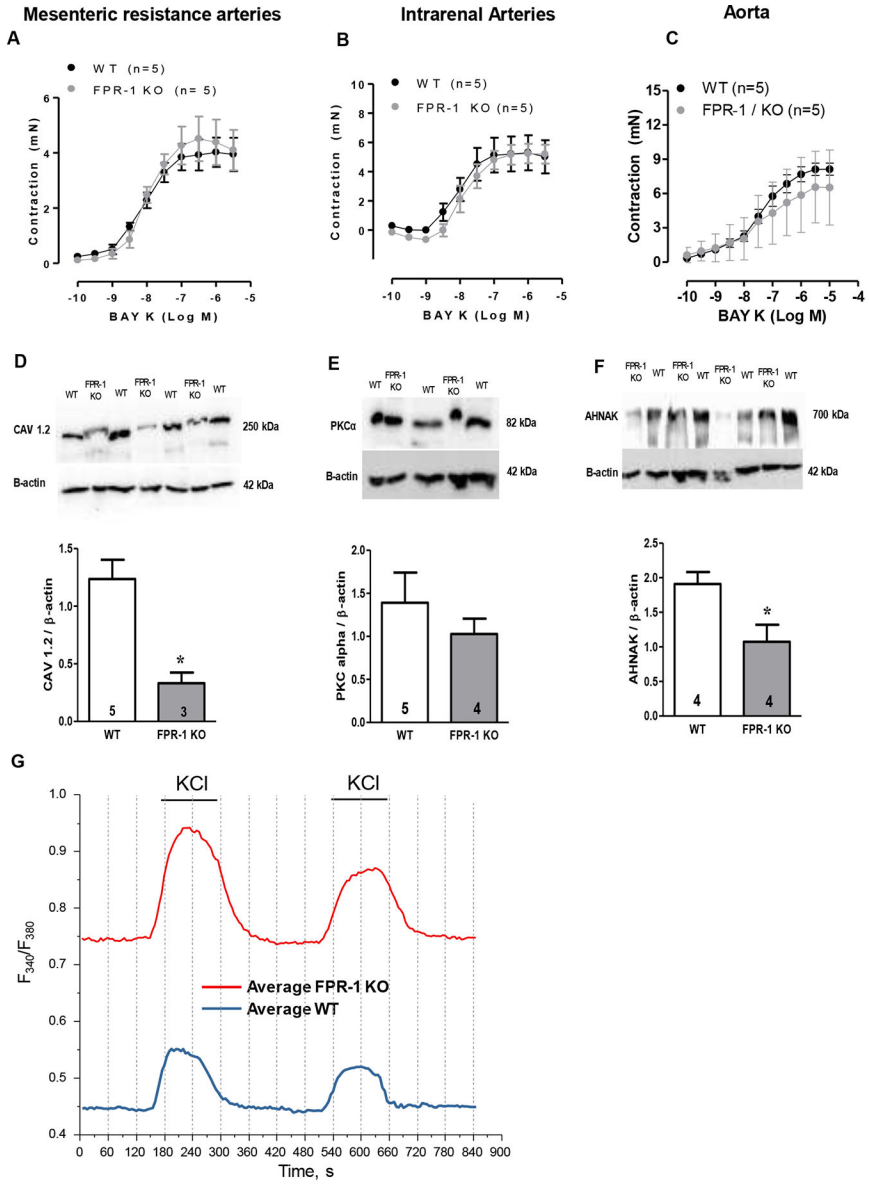

Figure 8.

Concentration-response curve to Bay K8644 (Bay K), L-type calcium channel (Cav 1.2) activator, in arteries from WT and FPR-1 KO mice (A, B and C). Representative blots (top) and densitometric analyses (bottom) from WT or FPR-1 KO in VSMCs for Cav 1.2 (D), PKCα (E), AHNAK (F) and β-actin. Number (n) of the animals used is indicated in the graphs. Student's t-test: *$p<0.05$ vs. WT. Single-cell intracellular Ca^{2+} measurements on fura-2-loaded VSMC showed that baseline intracellular Ca^{2+} concentration (absence of stimulus) is higher in VSMC from FPR-1-KO when compared to WT (G and table 1). KCl (120 mM) was used to induce Ca^{2+} influx (G and table 1).

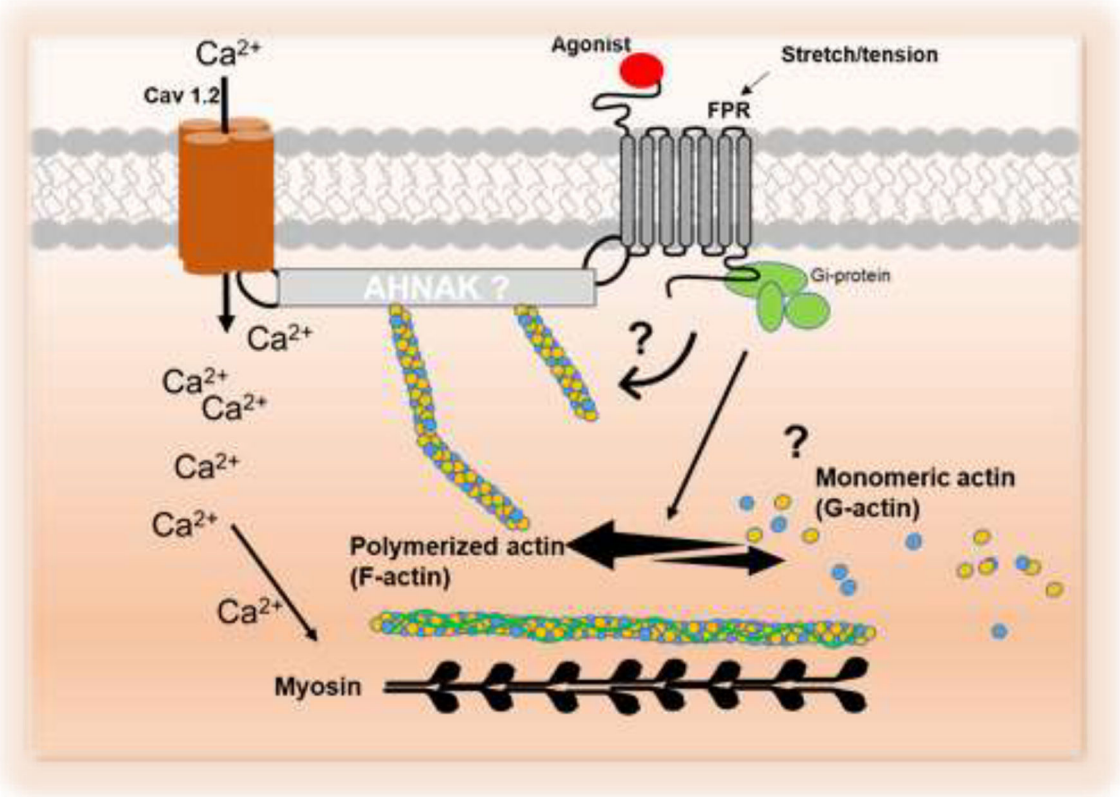

Figure 9.
Schematic demonstrating that formyl peptide receptor-1 (FPR-1) play a role in the vascular function.

Table 1:

	WT	KO	
n	14	18	
Baseline	0.44±0.015	0.73±0.042	*
ΔF1	0,1±0.008	0,2±0.0016	*
$\tau 1_{rise}$, S	17±1.7	25±1.6	*
$\tau 1_{decay}$, S	29±3.9	32±1.9	
ΔF2	0,075±0.009	0,12±0.001	*
$\tau 2_{rise}$, S	25±2.3	28±3.8	*
$\tau 2_{decay}$, S	27±3.2	33±2.2	
ΔF Recovery	75%	63%	-